Eddy Activity in the South Indian Ocean from ERS-1 Altimetry

Karen J. Heywood
School of Environmental Sciences, University of East Anglia, Norwich, NR4 7TJ, U.K.
email: k.heywood@uea.ac.uk
http://www.uea.ac.uk/~e280/karen.htm

Yenamandra K. Somayajulu
National Institute of Oceanography, Dona Paula, Goa 403 004, India
email: yksoma@csnio.ren.nic.in

Abstract

Sea level anomalies from ERS-1 altimetry data have been used to calculate eddy kinetic energy (EKE) in the South Indian Ocean (10-40° S, 30-120° E). A significant proportion of the sea level variability is caused by the passage of westward propagating Rossby waves, which will be briefly mentioned. The EKE fields are used to investigate the seasonal changes in the eddy distributions. The clearest annual signal is in the Leeuwin Current, which displays markedly higher eddy energy in austral winter than in austral summer. The South Equatorial Current shows high energy at 10-20° S, strongest in winter. To the east of Madagascar, low EKE is seen to the west of the point at which the South Equatorial Current branches: the northern branch passing around the northern tip of Madagascar, while the southern branch becomes the eddy rich East Madagascar Current, which is markedly more variable in winter. Wind fields from the ERS-1 scatterometer enable us to study seasonal changes in the wind stress curl field, which influence the patterns of the EKE.
Keywords: altimetry, scatterometry, eddy kinetic energy, seasonality

Introduction

Sea level anomalies from ERS-1 altimetry data have been used to calculate eddy kinetic energy (EKE) in the South Indian Ocean (10-40° S, 30-120° E). Figure 1 shows the bathymetric features of the region. Two large meridional ridges divide the ocean into 3 basins: the Central Indian Ridge at ~70° E and the Ninety East Ridge at ~90° E. The westerlies (near 40° S) and the Trades (near 15° S) are strong in the South Indian Ocean compared to other oceans, and hence strong wind stress curl (WSC) exists between them, driving the subtropical gyre.

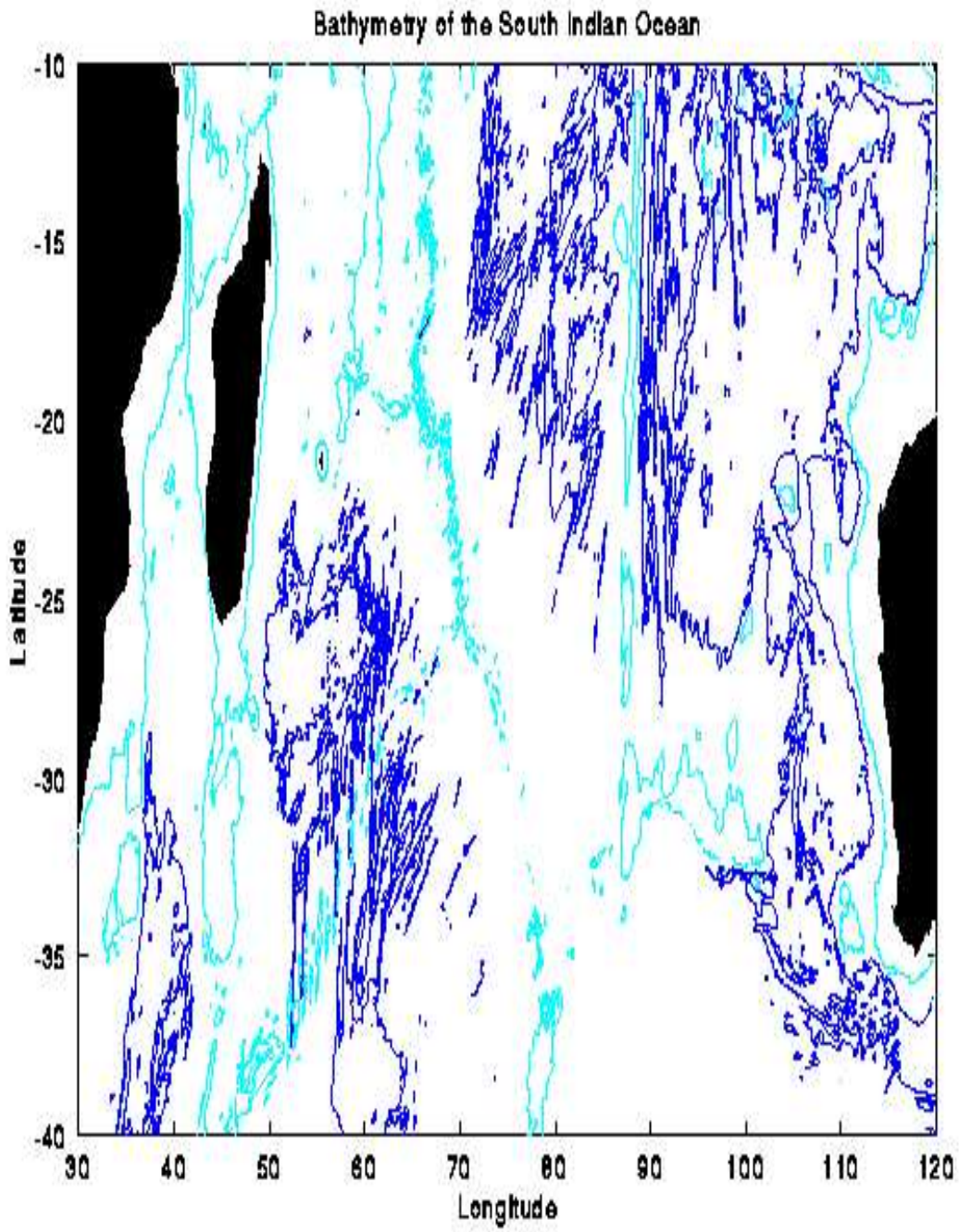

Figure 1. Bathymetry of the South Indian Ocean. The 2500 m contour (light blue) and 5000 m contour (dark blue) are shown.

The South Equatorial Current (SEC) flows westwards at about 10° S to the Mozambique and Madagascar Current systems which feed the Agulhas Current. The Agulhas Current system has one of the strongest mass transports of any western boundary current. The variability of the eastern Indian Ocean is unusually large for a eastern boundary domain. The large along-shore pressure gradient in the eastern Indian Ocean is a direct result of the presence of lower density water of Pacific origin to the north. Although the annual mean wind forcing is equatorward, the surface Leeuwin Current flows poleward against the prevailing winds which is attributed to thermal circulations driven remotely by Pacific heating and winds (Godfrey and Weaver, 1991; Morrow and Birol, 1997).

Data and Analysis

The processed ERS-1 sea level anomalies, provided on CD-ROM by AVISO, were used in this analysis. This is a validated altimetric data set with all environmental and orbit error corrections applied; orbits have been improved by use of TOPEX/ POSEIDON crossovers. ERS-1 cycles 6 to 18 were available (October 1992 to December 1993). The along-track sea surface height (SSH) anomaly data were smoothed by a 5-point median filter. The SSH anomalies were gridded onto a 1° by 1° grid using Gaussian interpolation with a full width half maximum of 150 km and a search radius of 200 km. The along track slopes of SSH anomalies were used to calculate the eddy velocity. The square of the eddy velocity represents EKE if we assume isotropy.

Wind stress data were obtained from the ERS-1 scatterometer, gridded into monthly data sets on a 1° by 1° grid, available on CD-ROM from CERSAT. WSC data will be considered.

Results and Discussion

Gridded SSH anomalies for austral summer (January to March; Figure 2) and austral winter (July to September; Figure 3) show two phenomena. First, the seasonal heating (the steric effect) leads, on average, to positive anomalies of a few tens of centimetres over the whole region in summer and negative anomalies in winter. Second, SSH anomalies around 10-20° S are dominated by large scale coherent variations: Rossby waves. Rossby waves in this region with primarily an annual period were described by Perigaud and Delecluse (1992) using Geosat data. The ERS-1 data confirm that the wave amplitude has a maximum of ~12 cm at ~90° E, 12° S, and that propagation is westward.

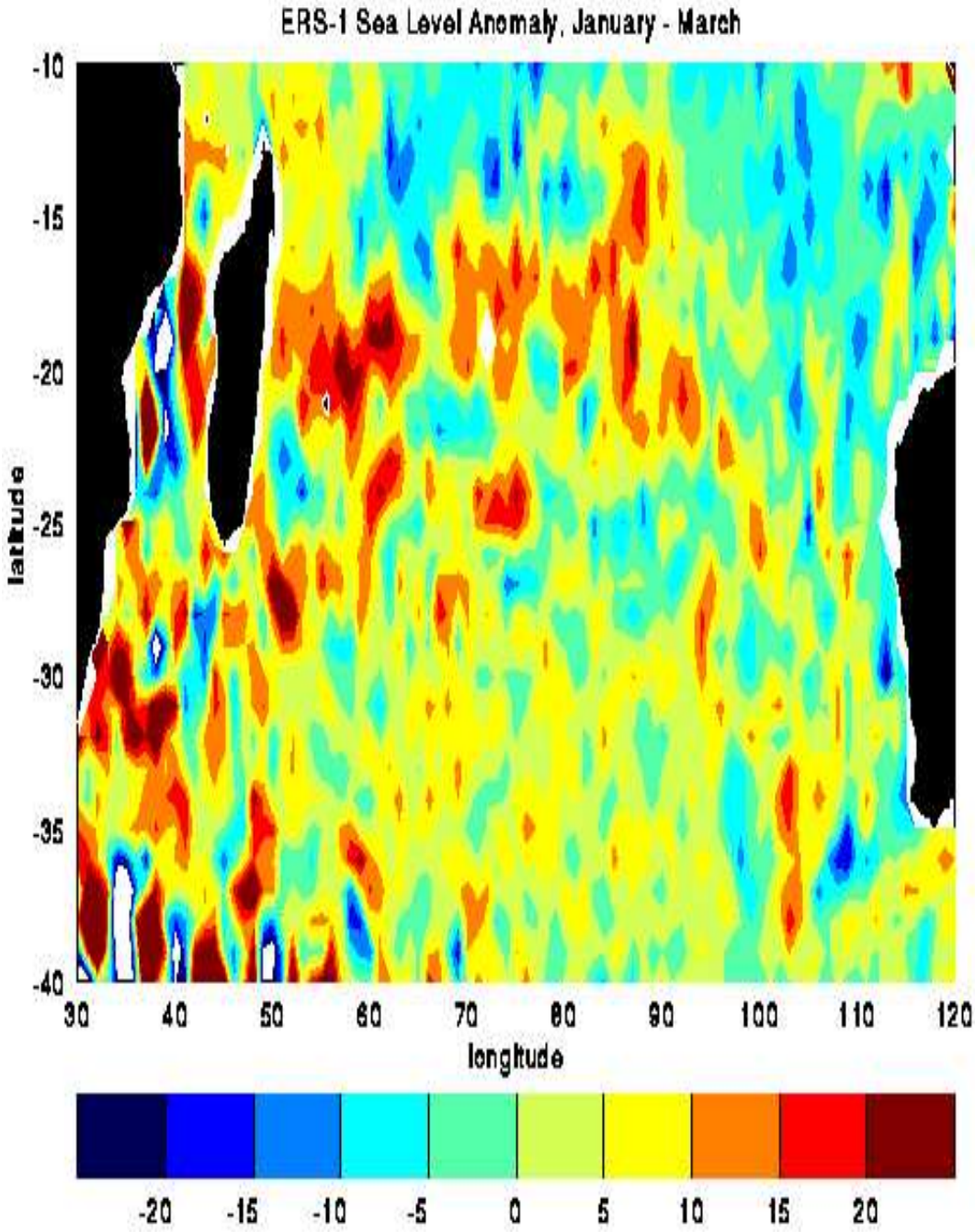

Figure 2. Sea level anomaly data (cm), January-March 1993, from the ERS-1 altimeter.

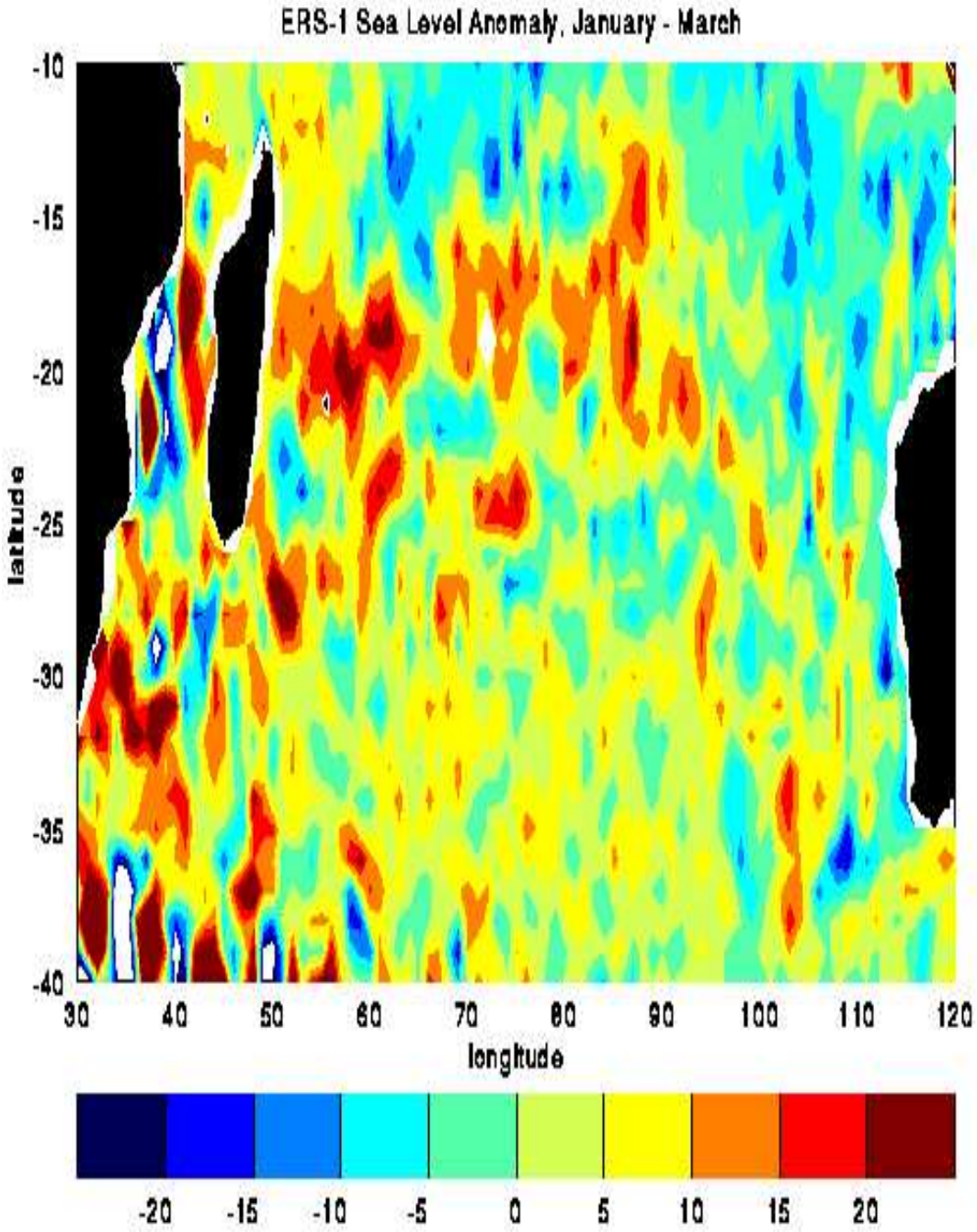

Figure 3. Sea level anomaly data (cm), July-September 1993, from the ERS-1 altimeter.

SSH variability (Figure 4), which simply considers variations in height, will represent the Rossby waves as well as variations due to meandering fronts and mesoscale eddies. These may be compared with the maps derived by Park and Gamberoni (1995) from TOPEX/POSEIDON data. They obtained values of 8-10 cm in the SEC, up to 18 cm in the Mozambique Current, 30 cm in the Agulhas Return Current, and 10 cm in the Leeuwin Current. In the ERS-1 data, peak values are a little larger, particularly in the Leeuwin and Mozambique Currents, probably because TOPEX/POSEIDON data are too widely spaced to analyse the eddy fields, so require more smoothing.

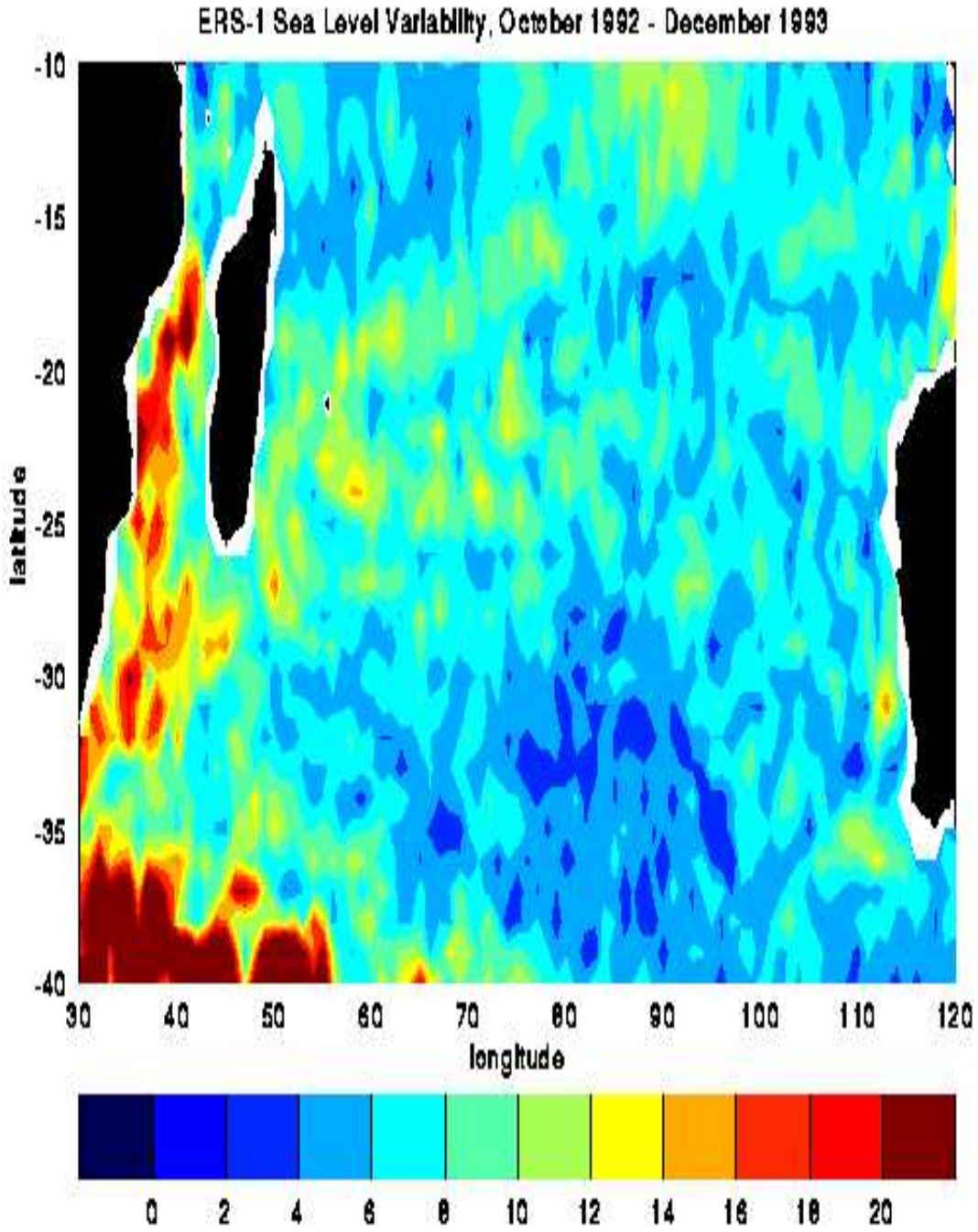

Figure 4. Root mean square sea level anomaly (cm), October 1992 - December 1993, from ERS-1 altimeter.

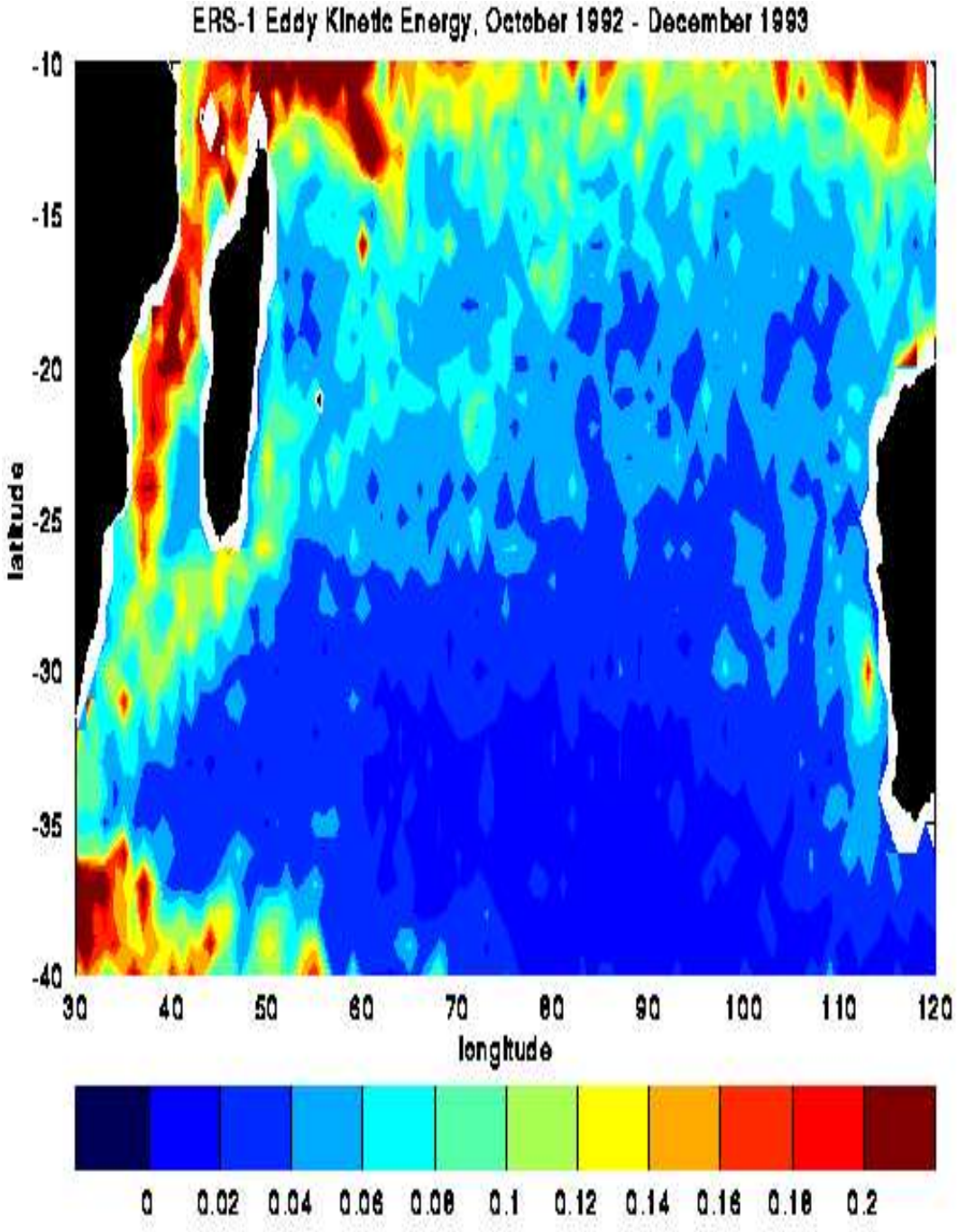

Figure 5. Mean eddy kinetic energy ($m^2 s^{-2}$), October 1992 - December 1993, from ERS-1 altimeter.

Since EKE is derived from the sea surface slope, it is indicative of variations in geostrophic velocity, and therefore more accurately shows the eddy field and frontal movement (Figure 5). Notice that since the months of October to December are included twice, these mean maps will be biased towards the austral spring months. While both the SSH variability and the EKE show the very highly variable regions such as the Agulhas Return Current and the Mozambique Current, there are significant differences, particularly in areas where the Rossby wave activity is large. We shall therefore concentrate on the EKE.

EKE values in the centre of the subtropical gyre are low, less than 0.02 $m^2 s^{-2}$, as would be expected in what are often called 'eddy deserts'. The northernmost region, around 10° S, marks the axis of the SEC, and exhibits high EKE, particularly in the far east close to the Indonesian Throughflow, and far west near the northern tip of Madagascar. The Mozambique Current is clearly a highly variable and eddy rich area, with EKE exceeding 0.2 $m^2 s^{-2}$. The *in situ* observations of Saetre and Jorge da Silva (1984) showed that the Mozambique Current was dominated by eddies, with a relatively small net transport. The Agulhas Return Current, which flows strongly east near 40° S, shows high EKE as far east as 55° E.

Notice the low EKE immediately east of Madagascar at 50-60° E, 15-20° S. This marks a quiescent area, where the SEC does not penetrate. The path of the SEC is zonal until about 60° E, where it branches; one branch turns to the north around the tip of Madagascar, while a second branch turns to the south as the East Madagascar Current. It is suggested that this branching is prompted by the Central Indian Ridge, since it takes place immediately after the SEC crosses this prominent feature at about 65° E. Note also that the two branches follow lines of constant WSC (Figure 6).

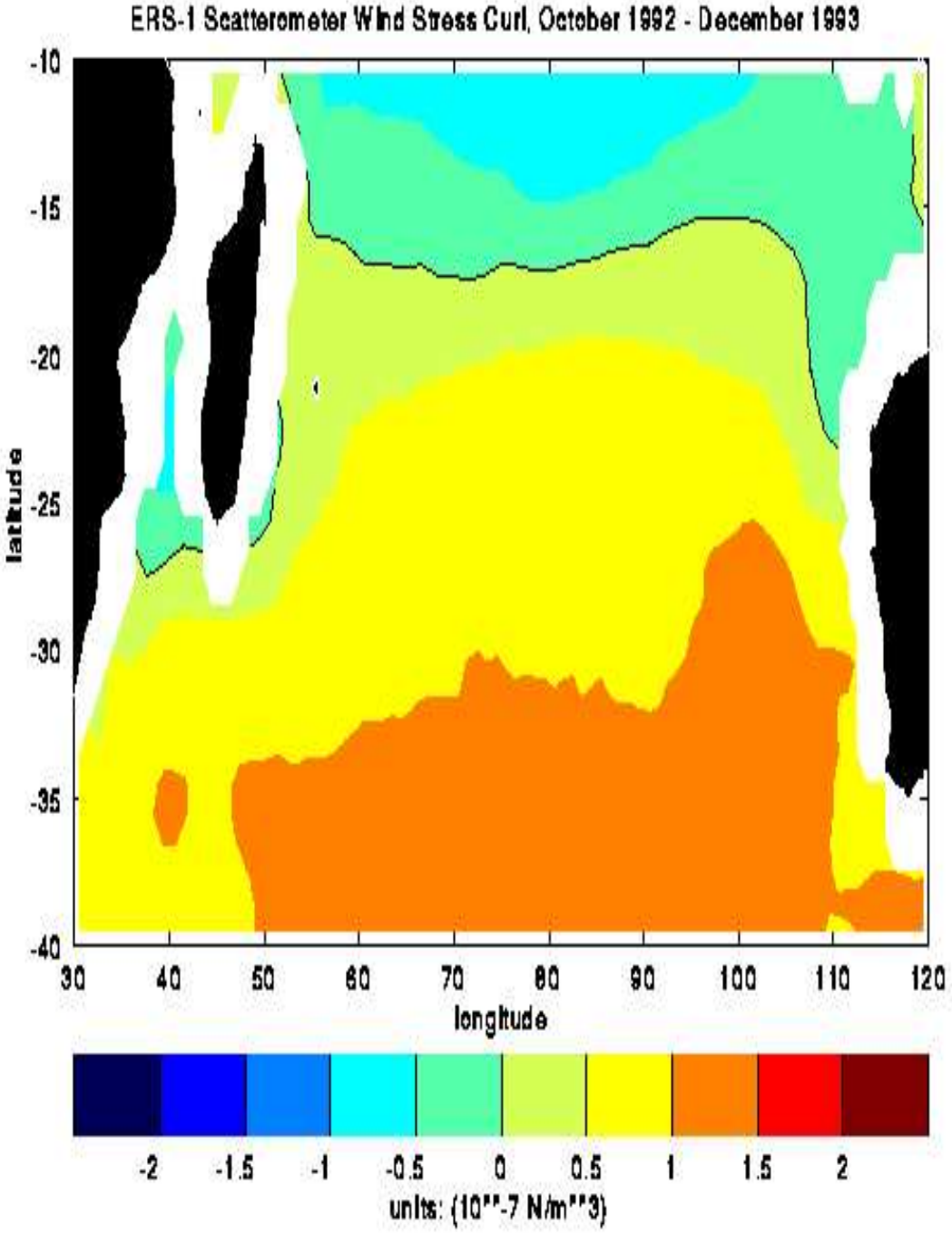

Figure 6. ERS-1 scatterometer wind stress curl (10^{-7} N m^{-3}). This is an average for the period October 1992 to December 1993 inclusive.

The East Madagascar Current exhibits high eddy variability. Drifting buoys (Lutjeharms *et al*., 1981) have shown that the East Madagascar Current is variable in its path, sometimes retroflecting, sometimes turning north around Madagascar (to return south eventually with the Mozambique Current along the African coast), and frequently generating cyclonic loops and eddies. These eddies are caused by the joint flow of the Mozambique and East Madagascar Currents over the Mozambique Ridge (Tomczak and Godfrey, 1994). The EKE clearly shows this area of high eddy activity from the East Madagascar Current to its confluence with the Agulhas Current at the African coast.

The west coast of Australia near 30° S is marked by higher EKE in the region of the Leeuwin Current, which flows to the south hugging the coastline. A further area of high EKE is located at the northwest corner of the continent, again very close to the coast, but this is on the very wide continental shelf and may be caused by tide model errors.

The mean scatterometer data for the same period show the forcing of the subtropical gyre (Figure 6), with negative WSC in the north, and positive WSC in the south. The maximum values are found at 35-40° S. The distribution is approximately zonal, with some deviation at the east and west boundaries to skirt Madagascar and Australia. The zero in WSC is located between 15 and 17° S for much of the region, although it is found at 27° S just south of Madagascar. The zero in WSC is ~5° further south than the main jet of the SEC. This is the region in which Sverdrup dynamics begin to change into equatorial dynamics.

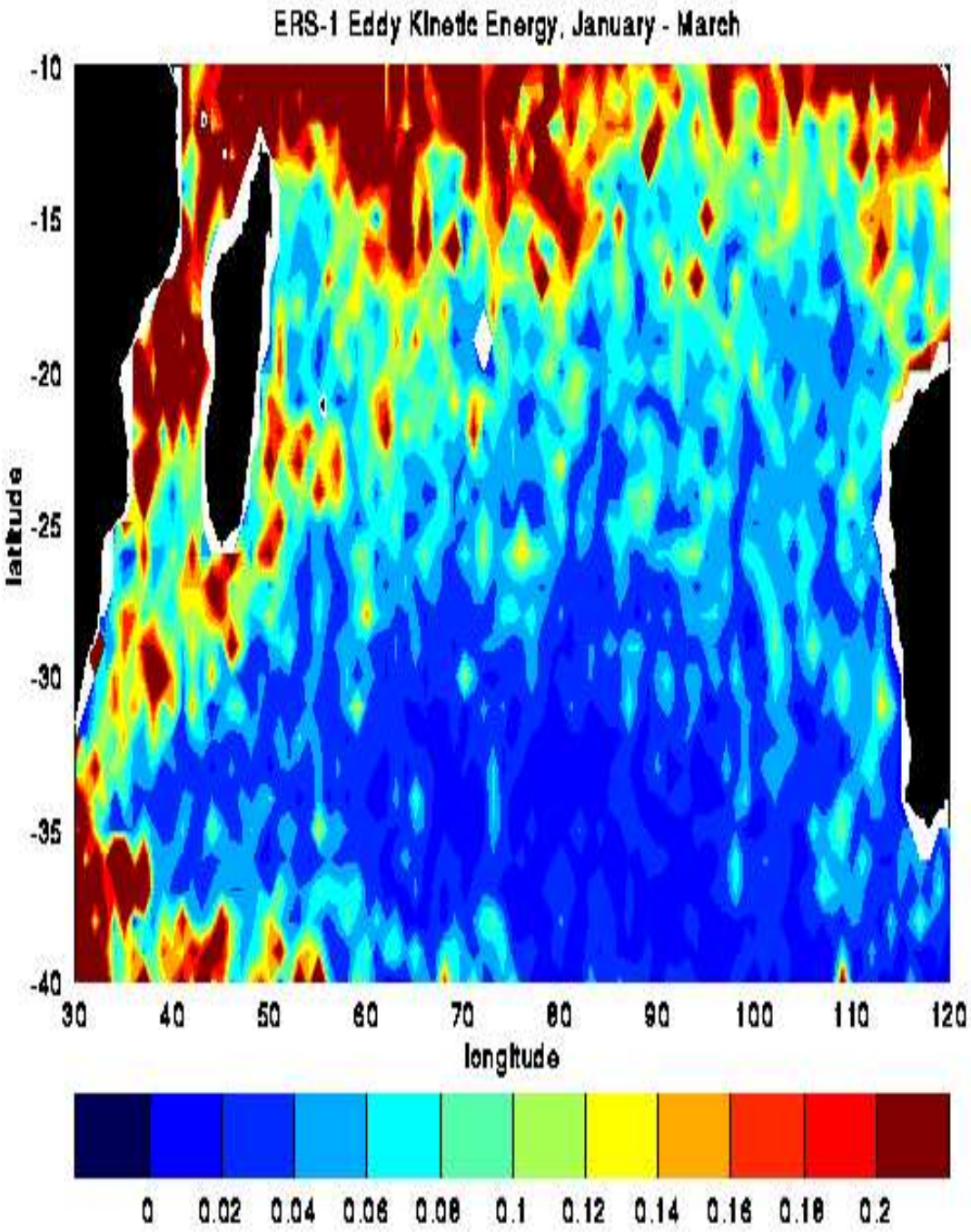

Figure 7. Eddy kinetic energy (m^2 s^{-2}) for the months of January-March 1993 (austral summer) from the ERS-1 altimeter.

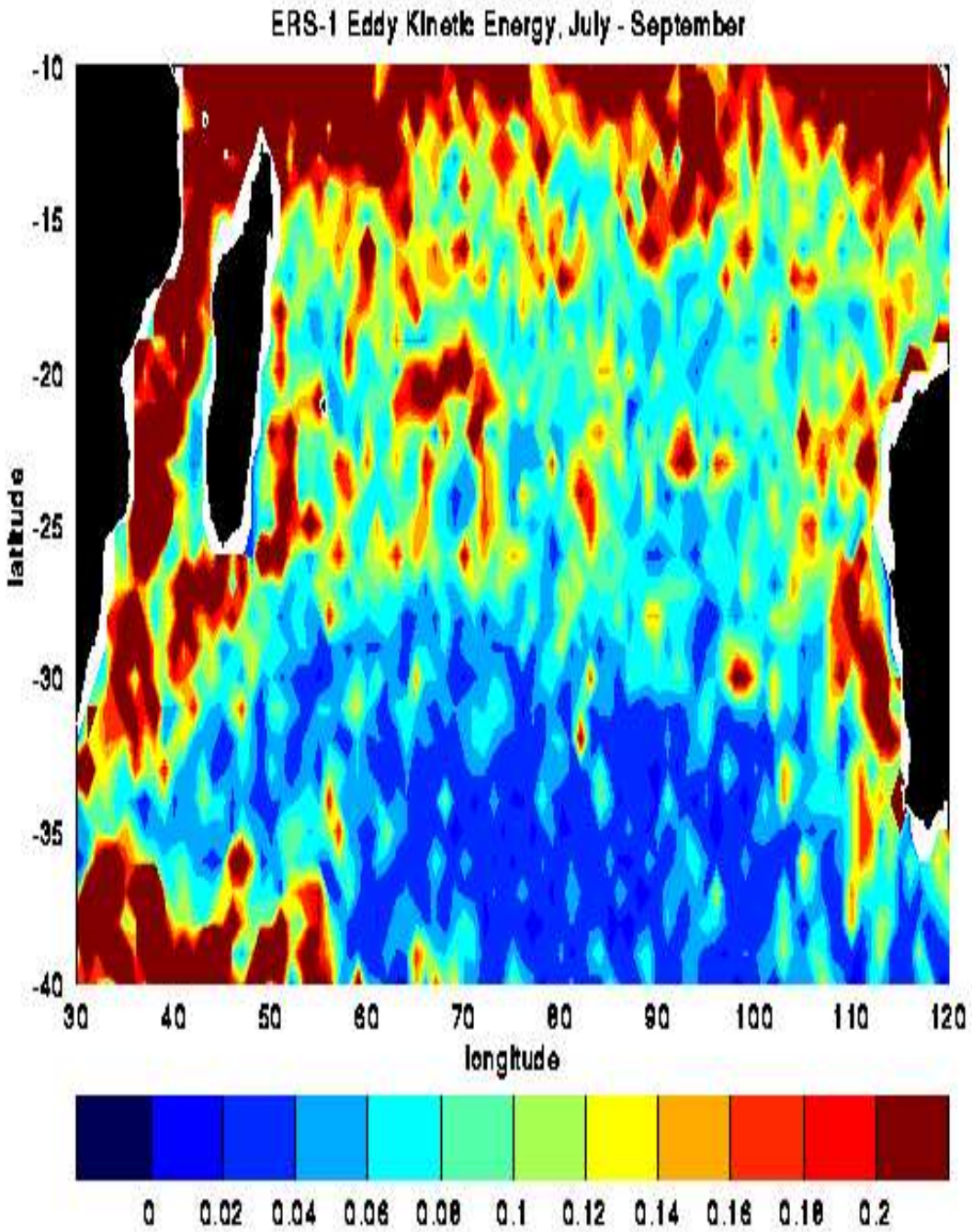

Figure 8. Eddy kinetic energy (m^2 s^{-2}) for July-September 1993 (austral winter) from the ERS-1 altimeter.

We consider now the seasonality of the EKE and WSC distributions. The 4 seasons considered are January-March (austral summer; Northeast Monsoon season), April-June (austral autumn), July-September (austral winter; Southwest Monsoon season) and October-December (austral spring, for which two years' data are available). Spring and autumn are the transitional periods in the monsoonal wind regime, so our main attention is focused on winter and summer. January-March (Figure 7) has lowest EKE over the region as a whole, as would be expected when the wind stress is least, whereas austral winter (Figure 8) exhibits the greatest EKE. This is similar to the seasonality observed over the subpolar North Atlantic (White and Heywood, 1995). Locally, however, there are seasonal changes which deserve more discussion.

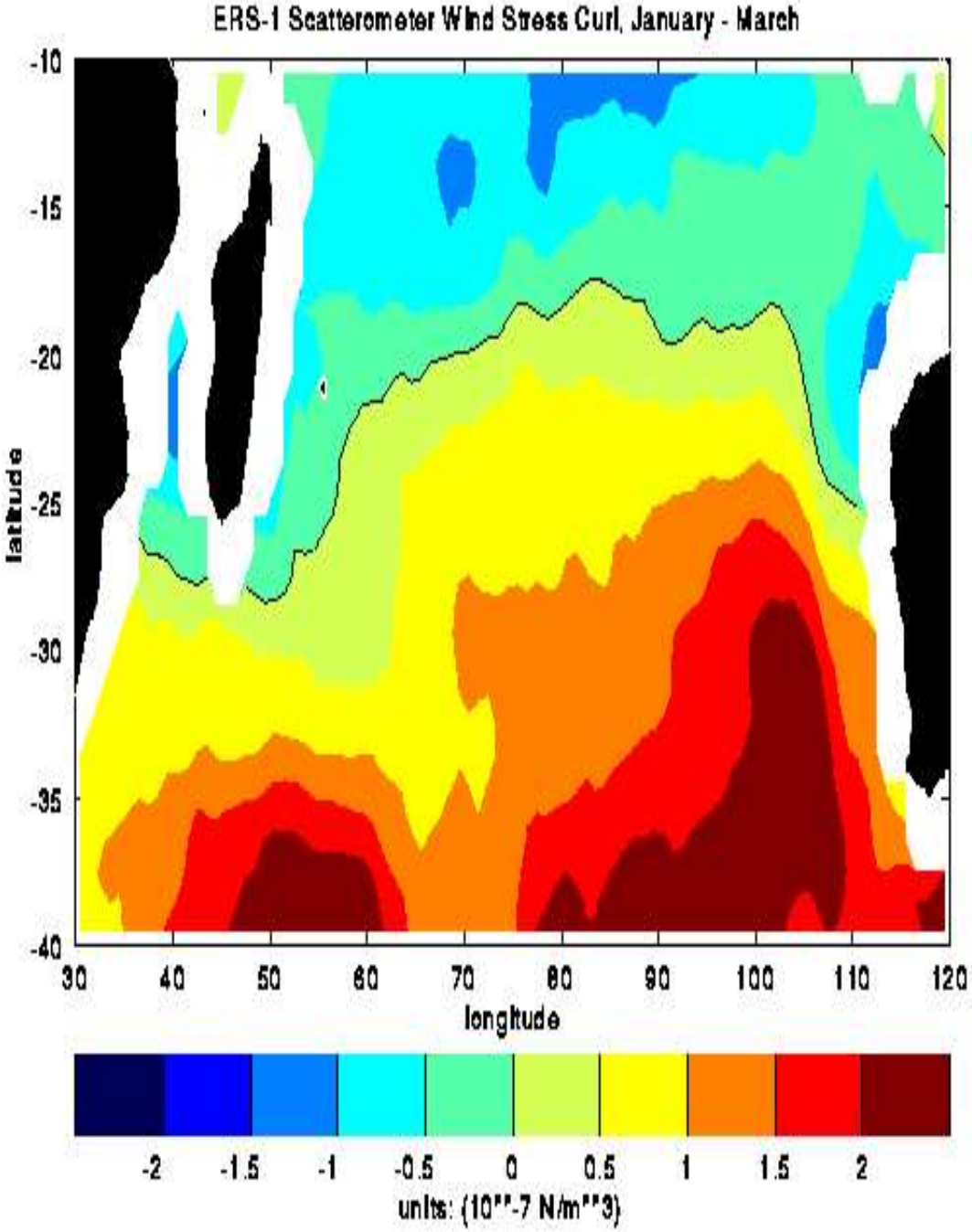

Figure 9. Wind stress curl (10^{-7} N m^{-3}) for the months of January to March 1993 (austral summer) from the ERS-1 scatterometer.

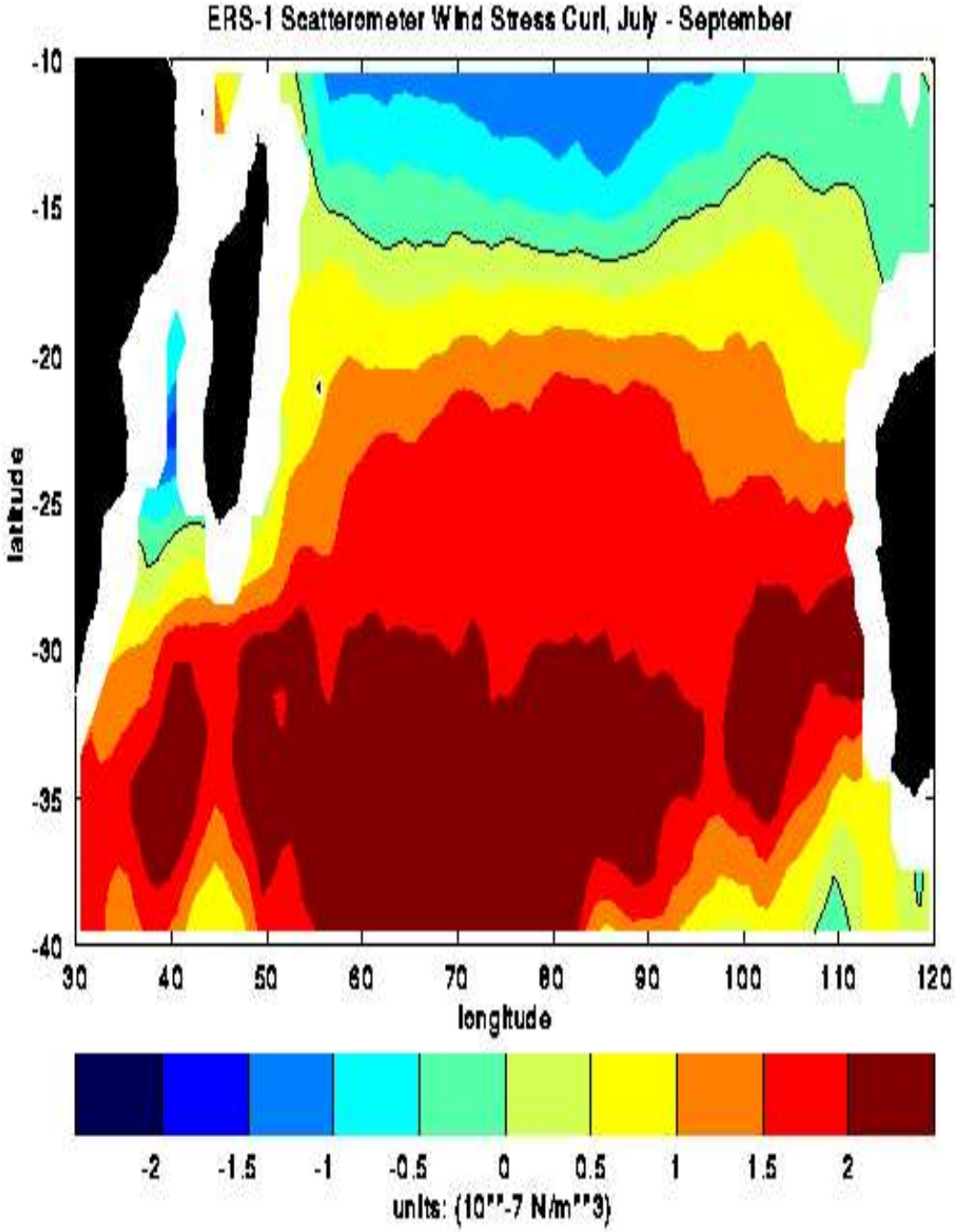

Figure 10. Wind stress curl (10^{-7} N m^{-3}) for the months of July to September 1993 (austral winter) from the ERS-1 scatterometer.

Drifter data in the South Indian Ocean (Molinari *et al.*, 1990) showed maximum westward speeds in the SEC in austral winter and spring, with the axis of flow between 8 and 16° S. Between July and September, the SEC expands north, reaching 6° S in September (Tomczak and Godfrey, 1994). Scatterometer data show the summer WSC distribution to be fairly smooth (Figure 9), whereas the sharpest gradient in WSC occurs, not surprisingly, in austral winter (Figure 10). The zero WSC is located slightly further north in winter than summer, but this does not appear to influence the location of the maximum in EKE, which extends, if anything, further south in winter than summer. The important influence is that in winter (the Southwest Monsoon season) the wind speed in the Trades is greater over the whole of the SEC (5-20° S). This leads to higher EKE, both indirectly by forcing the SEC faster which then is more inclined to baroclinic instabilities, and directly by generating eddies through fluctuating WSC. It is known that the SEC intensifies during the austral winter.

We saw earlier that the SEC splits into two just east of Madagascar. Swallow *et al.* (1988) observed that the transports in the two branches (30 Sv to the north and 20 Sv to the south) varied little over the year. In the altimetry, however, the EKE field is considerably stronger in the East Madagascar Current in winter than it is in summer.

The South Indian Ocean has been divided into 5 areas, based upon their oceanographic current regimes: SEC (10-20° S, 50-110° E), Leeuwin Current (20-35° S, 100-120° E), Subtropical gyre (25-40° S, 60-100° E), Mozambique Current (10-30° S, 30-50° E) and Agulhas Return Current (30-40° S, 30-50° E). EKE values during the 15 months of ERS-1 data are shown in Figure 11. Although the time series is shorter than we would prefer, it is possible to identify seasonal signals.

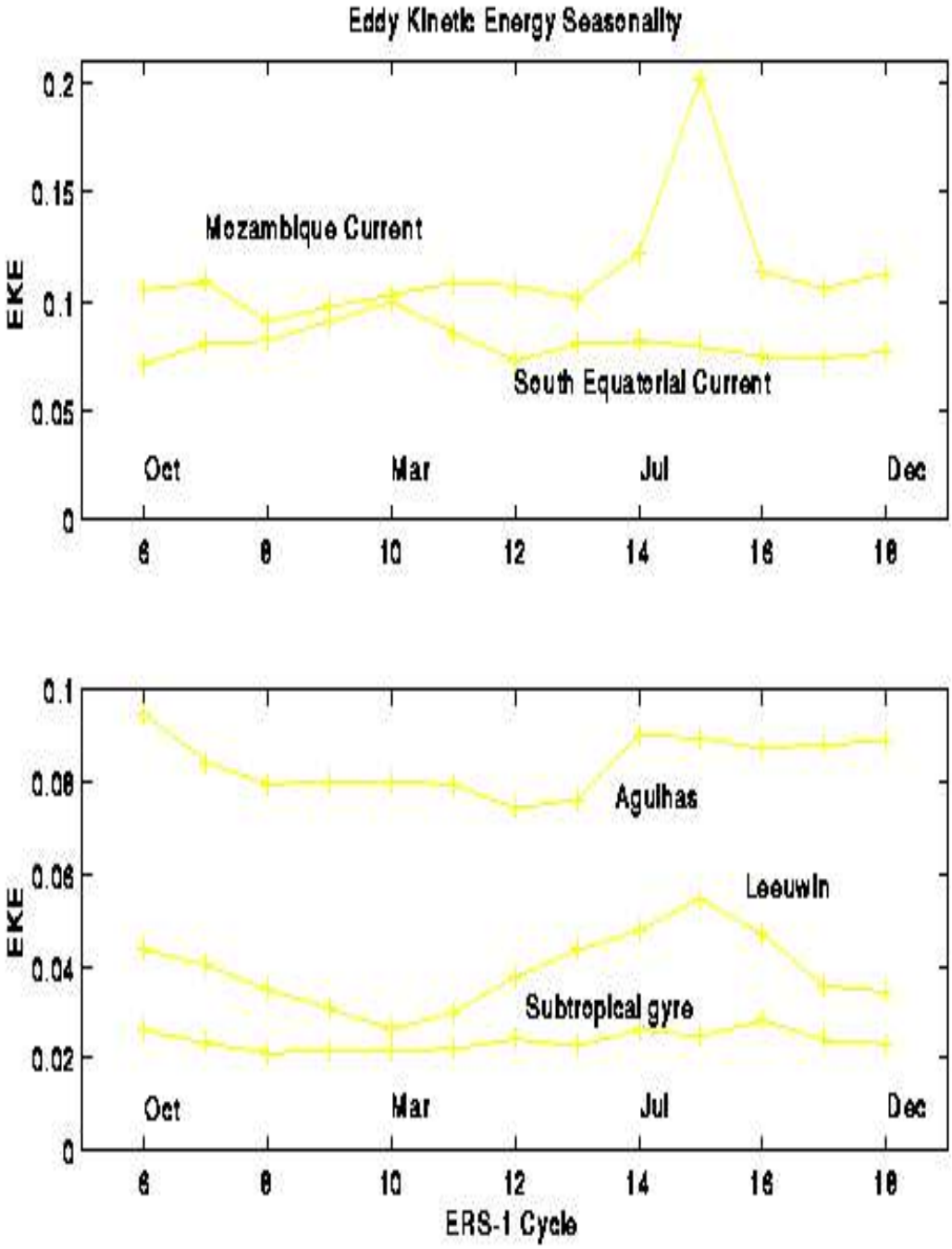

Figure 11. Eddy kinetic energy ($m^2 s^{-2}$) over 15 months from October 1992 to December 1993, for five different regions of the South Indian Ocean. Note the different vertical scales for upper and lower plots.

The most clear seasonal signal is in the Leeuwin Current, which peaks in August and has a minimum in March. This may be associated with local wind stress directly generating eddies, but it is likely also to be due to the strength of the Leeuwin Current, which peaks between May and July (Cresswell and Golding, 1980).

The Subtropical Gyre shows the same seasonality as the Leeuwin Current but an order of magnitude smaller. The Agulhas Current shows higher EKE in the second half of the year than in the first half of the year. The Mozambique Current also exhibits a peak in August, although since this is based upon only one year of data, it is not possible to say whether this is a regular seasonal signal. The SEC shows variations which may or may not be seasonally related.

Conclusions

The study of contemporaneous wind stress data from the ERS-1 scatterometer, and sea level data from the ERS-1 altimeter, has enabled us to study the seasonal signals in the eddy kinetic energy field of the South Indian Ocean. This is an area about which little is known, compared with the more accessible (to ships) and well-studied North Atlantic.

References

Cresswell, G. R. and T. J. Golding, 1980:
Observations of a southflowing current in the southeastern Indian Ocean. *Deep-Sea Res.*, **27**, pp. 449-466.

Godfrey, J. S. and A. J. Weaver, 1991:
Is the Leeuwin Current driven by Pacific heating and winds ? *Progr. Oceanogr.*, **27**, 225-272.

Lutjeharms, J. R. E., N. D. Bang and C. P. Duncan, 1981:
Characteristics of the currents east and south of Madagascar, *Deep-Sea Res.*, **28**, 879-899.

Morrow, R. and F. Birol, 1997:
Forcing mechanisms for the southeast Indian Ocean from TOPEX/POSEIDON altimetry and ERS1 scatterometry. Submitted to *J. Geophys. Res.*

Park, Y.-H. and L. Gamberoni, 1995:
Large scale circulation and its variability in the south Indian Ocean from TOPEX/POSEIDON altimetry. *J. Geophys. Res.*, **100**, 24911-24929.

Perigaud, C. and P. Delecluse, 1992:
Annual sea level variations in the southern tropical Indian Ocean from Geosat and Shallow water simulations. *J. Geophys. Res*., **97**, 20169-20178.

Perigaud, C. and P. Delecluse, 1993:
Interannual sea level variations in the tropical Indian Ocean from Geosat and shallow water simulations. *J. Phys. Oceanogr*., **23**, 1916-1934.

Saetre, R. and A. Jorge da Silva, 1984:
The circulation of the Mozambique Channel. *Deep-Sea Res.*, **31(5)**, 485-508.

Swallow, J. C., M. Fieux and F. Schott, 1988:
The boundary currents east and north of Madagascar 1. Geostropic currents and transports. *J. Geophys. Res*., **93**, 4951-4962.

Tomczak, M. and J. S. Godfrey, 1994:
Regional Oceanography: An Introduction. Pergamon, Oxford, 422pp.

White, M. A. and K. J. Heywood, 1995:
Seasonal and interannual changes in the North Atlantic subpolar gyre from Geosat and TOPEX/POSEIDON altimetry. *J. Geophys. Res*., **100**, 24931-24941.

Keywords: ESA European Space Agency - Agence spatiale europeenne, observation de la terre, earth observation, satellite remote sensing, teledetection, geophysique, altimetrie, radar, chimique atmospherique, geophysics, altimetry, radar, atmospheric chemistry